



CHARACTERIZATION OF ETHYL ACETATE-BASED LEAF EXTRACT OF *Entada rheedii* Spreng. BY USING LIQUID CHROMATOGRAPHY QUADRUPOLE TIME-OF-FLIGHT MASS SPECTROMETRY

Lekshmy R. Nair¹, M. Durairandian^{2*}, and Mini Gopinathan²

¹Department of Botany & Biotechnology, KVM College of Arts and Science (Affiliated to the University of Kerala), Kokkothamangalam, Cherthala, Alappuzha district - 688 527, Kerala (India)

²Department of Biotechnology, Vivekanandha College of Arts and Sciences for Women (Autonomous), Elayampalayam, Tiruchengode, Nammakkal - 637 205, Tamil Nadu (India)

*e-mail: drdurairandian@vicas.org

(Received 12 January, 2025; accepted 7 June, 2025)

ABSTRACT

Plants have certain important characteristics and different medicinal properties. From antiquity to the present day various plant parts such as leaves, stems, roots, rhizomes, flowers, tendrils, bulbs, etc., have been used in preparation of medicinal products. *Entada rheedii* Spreng. grows in tropical areas and its parts are used as remedies for different ailments. The present study was aimed to characterise the important chemical components of *E. rheedii* leaf extract by liquid chromatography combined with quadrupole-time-of-flight mass spectrometry (LC-MS-QTOF). This analytical approach enabled the identification of several bioactive flavonoids, including apigenin, genistein, kaempferol, as well as nicoflorin, astragalin, quercetin, and spiraeoside. The LC-MS-QTOF showed clear peaks corresponding to these compounds with retention times of 4.79 and 8.58 min. Uniform patterns of fragmentation have been used to confirm the structural identity of compounds. These flavonoids are recognized for their pharmacological properties, including antioxidant, anti-inflammatory, and anticancer effects. This study provided valuable insights into the phytochemical profile of *E. rheedii* leaf extract, aiding in the understanding of its potential medicinal uses.

Keywords: *Entada rheedii*, ethyl acetate extract, plant secondary metabolites, characterization, bioactivity analysis

INTRODUCTION

Entada rheedii Spreng. is known for its therapeutic properties in traditional African and Asian medicine. This tropical vine grows on the coasts and has been used for centuries to treat ailments like infections, inflammations, and sleep disorders. Despite its wide use, little is known about the plant's phytochemical composition, especially the biologically active substances responsible for its pharmacological effects. Previous studies have reported the presence of flavonoids in its bark (Shafaat-Al-Mehedi *et al.*, 2015), and several bioactive constituents such as tryptophan derivatives, triterpenoid saponins (rheediinoside A and B, tryptorheedei A and B), oleanane-type triterpene oligoglycosides (rheedeiosides A–D), and thioamide glycosides in seed kernels (Nzowa *et al.*, 2010; Sugimoto *et al.*, 2011; Taponjdjou *et al.*, 2013). Saponins, flavonoids, lectins, alkaloids, and phenolic acids are among the phytoconstituents that have been identified in Fabaceae species (Usman *et al.*, 2022). The phytochemical analysis of various extracts of *E. rheedii* leaves have shown the presence of flavonoids, glycosides, saponins, tannins, and terpenoids as determined by a phytochemical

examination, which also demonstrated that the leaves had strong antioxidant potential (Nair and Balasubrahmanian, 2023). Plants belonging to genus *Entada* are regarded as important and valuable sources of bioactive compounds (Salim *et al.*, 2024). However, there is knowledge gap regarding the phytochemical constituents of *E. rheedii* leaf extracts. Considering the plant's pharmacological potential and the likely presence of flavonoids, phenolic acids, and other bioactive substances in its leaves, a thorough chemical analysis is essential. The leaves of *E. rheedii* may also have useful medicinal qualities because these compounds are frequently linked to hepatoprotective, anti-inflammatory, and antioxidant effects.

Liquid chromatography combined with quadrupole time-of-flight mass spectrometry (LC-MS-QTOF) is a potent analytical tool frequently employed in the study of natural products. It is perfect for identifying a wide variety of secondary metabolites and profiling intricate plant matrices due to its high resolution, sensitivity, and mass accuracy (Colby and Lynch, 2018). Long *et al.* (2023) conducted a UPLC-QTOF-MS-based untargeted metabolomic and chemometric analysis of *Acer truncatum* leaves (ATL), collected from twelve locations across four climatic zones in Northern China, and identified 64 phytochemicals, including 34 newly reported from ATL, primarily flavonoids (FLAs) and gallic acid-containing natural products. The phytochemical composition and biological activities of *Anodendron parviflorum* leaf extracts using LC-MS/MS-QTOF analysis identified a wide array of bioactive compounds, including phenols, flavonoids, alkaloids, terpenoids, and saponins in the ethanolic extract (Sharmila and Selvaraj, 2024). In past decade, quadrupole time-of-flight mass spectrometry has drawn a lot of interest as this analytical method can handle the difficulties of a quickly evolving drug landscape (Allen and McWhinney, 2019).

Despite the long standing traditional uses of *E. rheedii*, a comprehensive phytochemical profiling of its ethyl acetate leaf extract from the specific geographical region of Kerala, India, using advanced LC-QTOF-MS/MS, has largely remained unexplored. This study was aimed to bridge this knowledge gap by providing a detailed chemical characterization of the extract, thereby offering scientific support for its traditional applications and highlighting its potential as a source for novel pharmaceutical agents.

MATERIALS AND METHODS

Chemicals and reagents

Hexane, ethyl acetate, methanol, acetonitrile (HPLC grade) and formic acid (analytical grade) were purchased from Merck Life Science Pvt. Ltd. (Mumbai, India). HPLC-grade water was obtained from a Milli-Q purification system (Merck Millipore, India). A 0.22 µm syringe-driven nylon 66 filter (AXIVA, India) was used for sample filtration before LC-MS analysis. Nitrogen gas, for desolvation in mass spectrometry, was supplied by Linde India Ltd. (Mumbai, India). All the solvents and reagents used were of analytical or HPLC grade and used without further purification.

Collection of plant materials

Entada rheedii plant materials were collected from the Karulai forest range in Kerala's Malappuram district in December 2019. After its authentication, the specimens were deposited in the Environmental Resources Research Centre's Herbarium in Thiruvananthapuram, Kerala (collection No: 8976). The leaves were separated, then washed with water and left to dry in the shade.

Sample preparation

Shade-dried leaves of *E. rheedii* were powdered and subjected to successive Soxhlet extraction using the solvents of increasing polarity: hexane, ethyl acetate, methanol, and water. Each extraction was continued until the solvent in siphon tube turned colourless, indicating exhaustive extraction. The extracts were then concentrated under reduced pressure. Among these, the ethyl acetate extract exhibited the most promising biological activity in preliminary screening and was, therefore, selected

for further phytochemical characterization. For LC-MS QTOF analysis, a portion of dried ethyl acetate-based leaf extract of *E. rheedii* was reconstituted in HPLC-grade methanol (Merck, Germany). The solution was then filtered through a 0.22 μm syringe-driven nylon 66 filter (Axiva, India) to remove particulates before injection into the LC-MS system.

Characterization using LC-MS QTOF

Phytochemical profiling of ethyl acetate-based leaf extract was performed using a Waters Xevo G2 QT of mass spectrometer coupled with a Waters Acquity UPLC system (Waters Corporation, Milford, USA) as per the method described by Ali *et al.* (2021). The UPLC system included a quaternary solvent manager (model H12QSM632A), a sample manager FKN (model K12SD1069G), a column chamber (model J12CHA730G), and a TUV detector (model J12TUV750A). Chromatographic separation was carried out by reversed-phase BEH C18 column (50 mm \times 2.1 mm, 1.7 μm particle size) (Waters Corporation, Milford, USA). The mobile phase consisted of water and acetonitrile with 0-1% formic acid, applied in gradient mode. The flow rate was maintained at 0-0.3 mL min⁻¹, and the injection volume was 10 μL . Electrospray ionization (ESI) was performed in both positive and negative ionization modes. The mass spectrometer operated over a scan range of m/z 50-1000. The source temperature was set at 350°C, with a desolvation gas flow rate of 900 L h⁻¹. Collision energy for MS/MS analysis ranged from 5 to 30 eV. Instrument control and data acquisition were performed using Mass Lynx software version 4.1 (Waters Corporation).

Each sample was analysed in triplicate to ensure reproducibility and accuracy of metabolite detection. The identity of compounds was determined based on high-resolution mass spectra, isotopic distribution patterns, and MS/MS fragmentation data. Tentative identification of compounds was performed by comparing the acquired spectra with the compound data available in PubChem database for respective compound CID entries.

RESULTS AND DISCUSSION

The application of liquid chromatography coupled with quadrupole time-of-flight mass spectrometry (LC-QTOF-MS) has proved instrumental in the precise identification and comprehensive characterization of the compounds present in the ethyl acetate extract of *E. rheedii* leaves. Accurate mass measurements and comprehensive full-scan MS/MS data were systematically acquired for key compounds, facilitating their structural elucidation. Elemental formulae were rigorously assigned based on exact mass data, and the identities of these compounds were further corroborated by their characteristic fragmentation patterns observed in both positive and negative electrospray ionization (ESI) modes. This dual-mode ESI approach proved particularly advantageous in enhancing the detection and characterization of both polar and non-polar constituents in the complex extract.

The analysis in positive ion mode revealed a distinct LC-MS chromatogram characterized by prominent peaks eluting between retention times (Rt) of 3.04 and 7.18 min (Fig. 1). The most dominant peak, observed at Rt 6.43 min, exhibited a substantial base peak intensity (BPI) of 1.23e6, strongly suggesting the presence of a major compound. Additional significant peaks, indicative of other constituents in lower abundances, were noted at Rt 4.79, 6.01, 6.70, and 7.01 min. Further observations in ESI+ mode extended the overall elution range from Rt 4.79 to 8.58 min, with the most intense peak appearing at Rt 7.91 min (BPI 1.12 e7), signifying a highly abundant analyte (Fig. 2). The presence of co-eluting compounds between Rt 7.27 and 8.20 min suggested a series of chemically related structures, warranting further studies into their identities and potential structural relationships.

In contrast, the negative ion mode analysis (Fig. 3) presented a different chromatographic profile with peaks observed within the retention time range of 4.75 to 8.44 min. A particularly prominent signal was detected at Rt 4.75 min, which indicated the presence of major phenolic compounds often readily ionized in negative mode due to their acidic functional groups. Compounds eluting at later

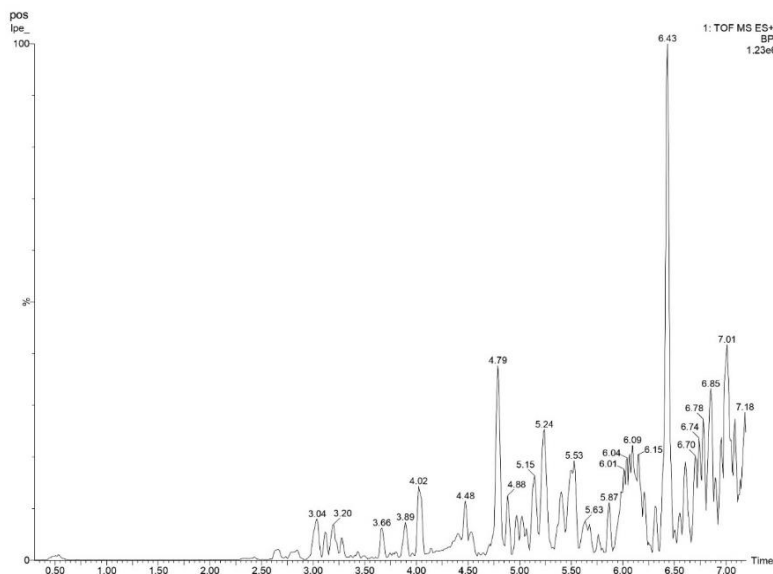


Fig. 1: LC-MS chromatogram of *Entada rheedii* ethyl acetate extract in positive ion mode showing base peak intensity across retention times. LC-MS chromatogram obtained in positive electrospray ionization mode displaying base peak intensity (BPI) across the retention times. Peaks indicate flavonoid and glycoside compounds.

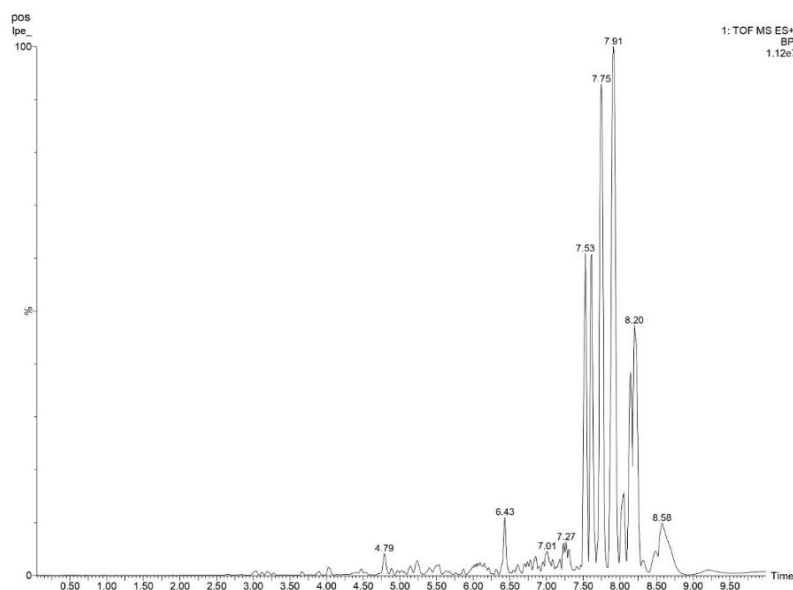


Fig. 2: LC-MS chromatogram of *Entada rheedii* ethyl acetate extract in positive ion mode displaying peaks between 4.79 to 8.58 min retention time; Expanded LC-MS chromatogram (positive mode) showing peaks between 4.79 to 8.58 min. The intense peak at 7.91 min indicates high analyte abundance.

retention times, specifically at Rt 7.37 and 8.44 min, were likely more lipophilic. This observation is consistent with the expectations for non-polar or glycosylated metabolites, which, despite sharing similar chemical structures, can exhibit varying polarities based on their degree of glycosylation or other structural modifications.

The complex chromatographic profiles observed in both positive and negative ion modes unequivocally confirmed the rich and diverse phytochemical composition of *E. rheedii* ethyl acetate-based leaf extract. The analyses strongly suggested the presence of various classes of compounds, including flavonoids, glycosides, and other phenolic compounds, which are commonly found in plant extracts known for their medicinal properties. Mass spectrometry (MS) proved invaluable in providing detailed molecular insights by precisely measuring the mass-to-charge ratio (m/z) of the ionized molecules (El Sayed *et al.*, 2020). This technique offers unique molecular fingerprints, revealing not only the molecular weights but also the characteristic fragmentation patterns (Gupta *et al.*, 2023), which are essential for analysing the natural extracts containing a wide array of compounds

such as flavonoids, alkaloids, and phenolics. The MS spectra consistently revealed several compounds characterized by significant peaks for both parent and fragment ions in both ESI modes.

High-resolution LC/MS analysis leverage the inherent sensitivity of LC-MS/QTOF system, and enable the detection of compounds even at trace levels (Gupta *et al.*, 2023). This technique provided

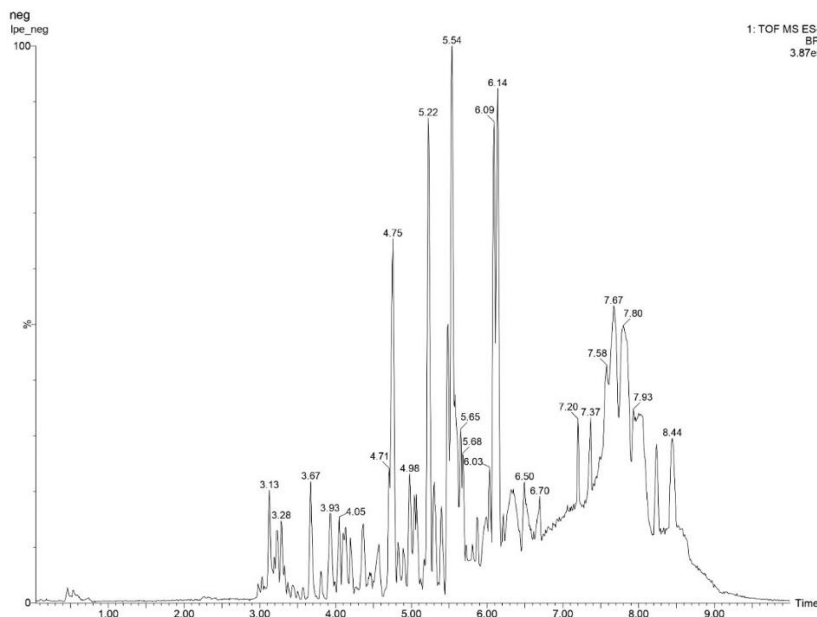


Fig. 3: LC-MS chromatogram of *Entada rheedii* ethyl acetate extract in negative ion mode displaying base peak chromatogram. The chromatogram displays multiple prominent peaks between retention times of 3.13 and 8.44 min, indicating the presence of diverse phytochemicals including flavonoids, glycosides, and phenolic compounds. The most intense peak is observed at Rt 5.54 min.

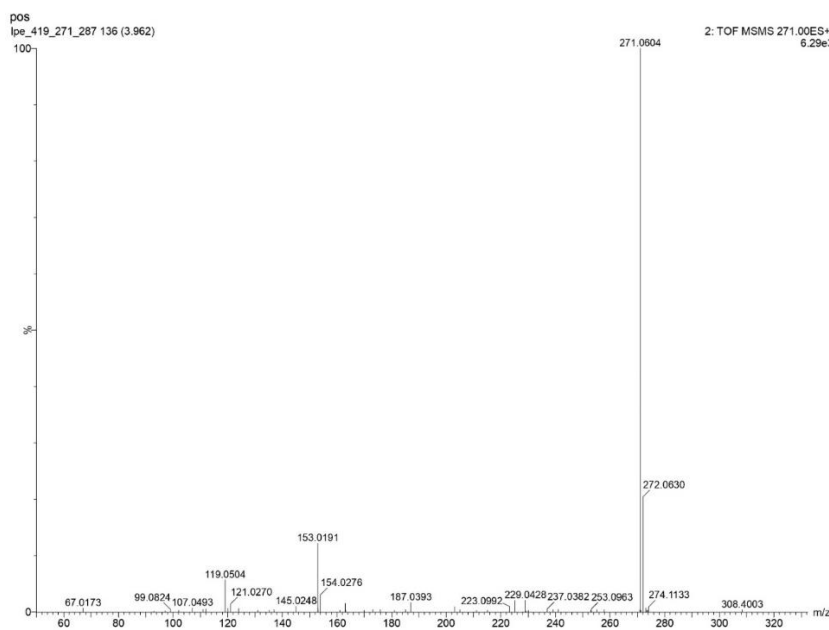


Fig. 4: MS/MS spectrum of apigenin (m/z 271.0604) identified in the ethyl acetate extract of *Entada rheedii* leaf; The MS/MS spectrum of apigenin (m/z 271.0604) acquired in positive ion mode. Diagnostic fragments at m/z 153 [Retro-Diels-Alder (RDA) cleavage] and m/z 121 support identification.

conclusive evidence for their molecular identities by comparing the observed fragment ions with the established spectral databases. Through this rigorous process, several key flavonoids were definitively identified based on their distinct molecular ions and characteristic fragmentation patterns. The identified compounds included quercetin, kaempferol, and genistein.

The Fig. 4 presents the spectrum of MS/MS analysis of a precursor ion with an accurate mass-to-charge ratio (m/z) of 271.0604. The spectrum was acquired in positive ion mode (ES^+). The protonated molecule's theoretical exact mass, 271.0601 Da, which is in close agreement with the precise mass measurement, indicated that the molecular formula was $C_{15}H_{10}O_5$. This formula is consistent with flavonoid compounds such as apigenin and genistein.

The fragmentation spectrum exhibited the characteristic fragment ions at m/z 153.0191 (base peak), 121.0270, and 119.0504. The dominant fragment at m/z 153 is indicative of Retro-Diels-Alder (RDA) cleavage, yielding the A-ring derived ion that is a well-established diagnostic for apigenin. Additionally, the fragment at m/z 121 corresponds to the hydroxybenzoyl cation

derived from the B-ring, while m/z 119 is another B-ring-derived fragment ion. The absence of an intense m/z 137 fragment, typically observed for genistein, further supports the identity of compound as apigenin (National Center for Biotechnology Information, 2025). Thus, the precursor ion mass accuracy combined with specific fragmentation pattern provides conclusive evidence for the presence of apigenin in the extract.

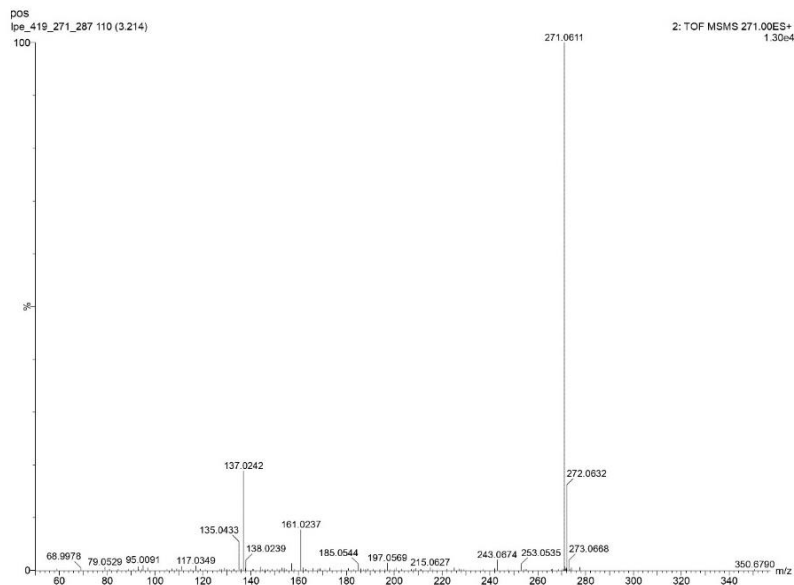


Fig. 5: MS/MS spectrum of genistein (m/z 271.0611) identified in the ethyl acetate extract of *Entada rheedii* leaf. Legend: MS/MS spectrum of genistein (m/z 271.0611) showing dominant fragment at m/z 137, diagnostic of genistein structure. [m/z – mass-to-charge ratio].

C-ring cleavage. Unlike apigenin which produces a base peak at m/z 153, the observed fragmentation pattern with m/z 137 as the most intense peak is diagnostic of genistein (National Center for Biotechnology Information, 2024). Therefore, the combination of accurate precursor mass and the distinctive base peak at m/z 137.0242 provides conclusive evidence for the presence of genistein in the extract.

Loliolide was identified with a molecular ion at m/z 197.1185 (Fig. 6). Its fragmentation yielded diagnostic ions at m/z 179.1076, 135.1183 and 162.0962, thereby confirming its identity and providing insights into its degradation pattern (National Center for Biotechnology Information, 2024). The spectrum showed a precursor ion that was obtained in positive ESI+ mode at m/z 196.00. The protonated molecular ion ($[M+H]^+$) of loliolide is most likely the source of strongest peak seen at m/z 197.1185, indicating that neutral molecule has a mass of 196 Da. The protonated molecular ion at m/z 197.1185 is the base peak, while a noticeable fragment ion can be seen at m/z 179.1076. This is equivalent to an 18 Da neutral loss ($197 - 179 = 18$ Da). The loss of a water molecule (H_2O) is frequently cited as the cause of neutral loss of 18 Da. This fragmentation pathway is highly prevalent for the compounds with hydroxyl groups, and aligns with loliolide's structure. M/z 135.1183, 161.0979, 180.1129, 133.1030, 162.0962, 107.0879, and 93.0716 are additional noteworthy fragments. A neutral loss of 62 Da ($197 - 135 = 62$) may be indicated by the fragment at m/z 135.1183. The compound's identification as loliolide, which has a hydroxyl group, susceptible to dehydration under ESI-MS/MS conditions, is strongly supported by the distinctive neutral loss of 18 Da (water). Quercetin showed a protonated molecular ion $[M+H]^+$ at m/z 303.0499 (Fig. 7). Its diagnostic fragments at m/z 137.0230, 153.0216, and 165.0210 support its well-known flavonoid structure (National Center for Biotechnology Information, 2025). The spectrum displays a precursor ion at

The LC-MS/MS spectrum of compound in Fig. 5 displayed a precursor ion at m/z 271.0611 $[M+H]^+$ in positive ion mode, which corresponds precisely to the protonated form of neutral molecular formula $C_{15}H_{10}O_5$ (theoretical $[M+H]^+ = 271.0601$ Da). This formula is consistent with the structures of flavonoids such as apigenin and genistein. Fragmentation analysis revealed a dominant base peak at m/z 137.0242. This fragment corresponds to $[C_7H_5O_3]^+$ with theoretical mass = 137.0239 Da, which is the characteristic fragment formed by RDA cleavage of genistein (an isoflavone). The fragment represents the A-ring portion of genistein after

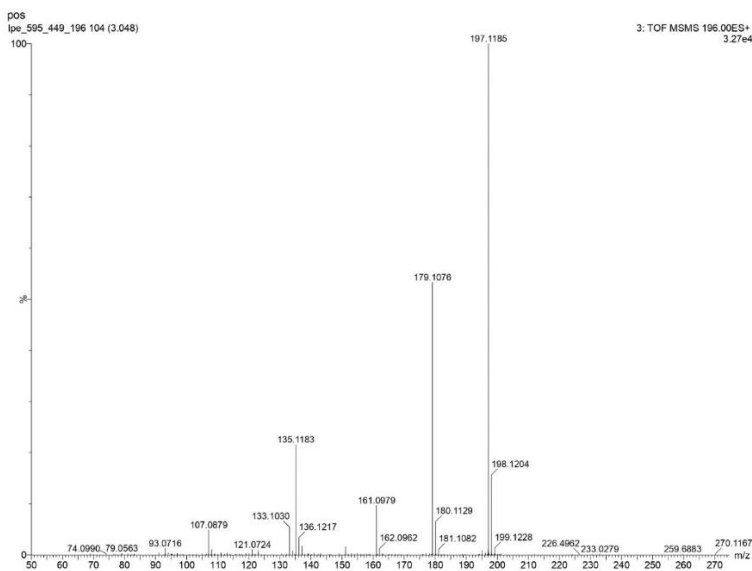


Fig. 6: MS/MS spectrum of loliolide (m/z 197.1185) identified in the ethyl acetate extract of *Entada rheedii* leaf. MS/MS spectrum of loliolide (m/z 197.1185) with characteristic neutral loss of 18 Da (water).

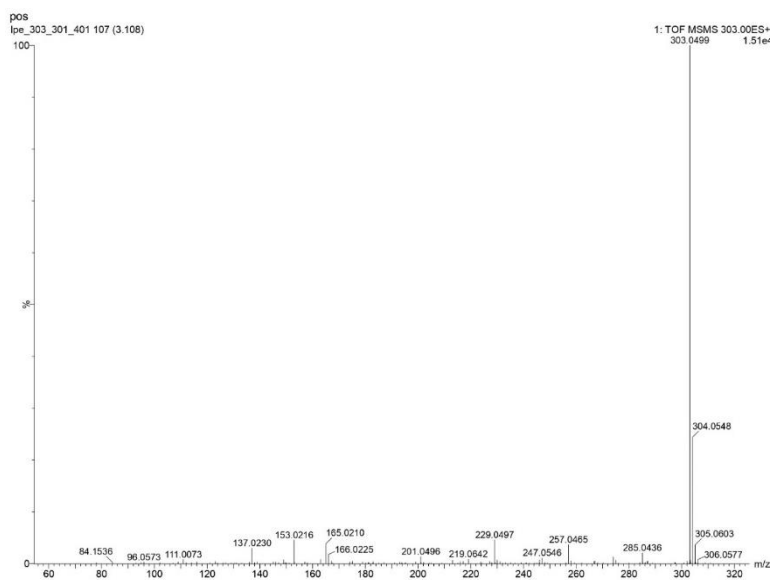


Fig. 7: MS/MS spectrum of quercetin (m/z 303.0499) identified in the ethyl acetate extract of *Entada rheedii* leaf. The spectrum shows a precursor ion at m/z 303.0499 ($[M+H]^+$) with characteristic fragment ions at m/z 285.0436 (loss of water, 18 Da), 153.0216, 137.0230, and additional minor fragments. The fragmentation pattern is consistent with the structural features of quercetin.

at m/z 303.0499, obtained in positive ESI+ mode. This m/z value is highly characteristic of quercetin ($[M+H]^+$). The base peak is the precursor ion itself at m/z 303.0499. Similar to genistein, this suggests high stability of the protonated molecule or low collision energy, as more extensive fragmentation is usually seen for flavonols like quercetin at higher collision energies (e.g., 30 eV). A notable fragment ion appears at m/z 285.0436, indicating the loss of a water molecule and a neutral loss of 18 Da ($303 - 285 = 18$ Da). This reflects common quercetin fragmentation. Another key fragment at m/z 153.0216 corresponded to a neutral loss of 150 Da ($303 - 153 = 150$ Da). This neutral loss is a familiar fragmentation pathway for quercetin. Additional fragments include m/z 257.0465, 229.0497, 165.0210, 137.0230, and 84.1536. The compound's identification as quercetin is strongly supported by the precursor ion at m/z 303 and the characteristic neutral losses of 18 Da (water) and 150 Da. These fragmentation patterns are well-established for this flavonoid.

The LC-MS/MS analysis revealed a precursor ion at m/z 433.0758 $[M-H]^-$, acquired in negative electrospray ionization (ESI-) mode (Fig. 8), corresponding to a deprotonated molecular formula of $C_{20}H_{18}O_{11}$. This formula suggests it a quercetin pentoside glycoside. The fragmentation spectrum showed a prominent base peak at m/z 301.0334, representing a neutral loss of 132 Da from the precursor ion ($433 - 301 = 132$ Da). This loss is characteristic of pentose sugars such as arabinose or xylose, confirming the presence of a quercetin

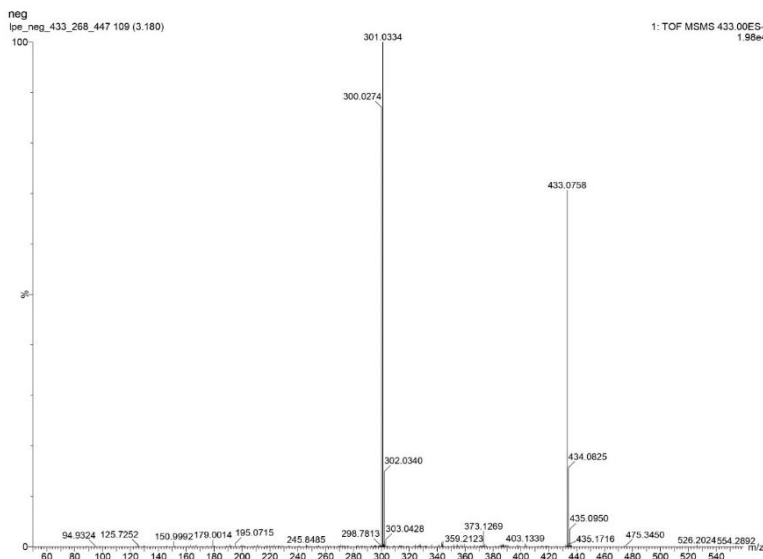


Fig. 8: MS/MS spectrum of avicularin (m/z 433.0758) identified in the ethyl acetate extract of *Entada rheedii* leaf. The spectrum shows a precursor ion at m/z 433.0758 ($[M-H]^-$) with a characteristic neutral loss of 132 Da, producing a major fragment ion at m/z 301.0334 corresponding to the quercetin aglycone. Additional minor fragments include m/z 300.0274 and 302.0340. The fragmentation pattern confirms the presence of a quercetin pentoside glycoside.

aglycone. The fragment at m/z 301 corresponds to $[M-H]^-$ of quercetin (theoretical m/z 301.0340 Da), further validating this identification. Minor fragments were also observed at m/z 300.0274 and 302.0340. Both avicularin (quercetin 3-O-arabinofuranoside) and reynoutrin (quercetin 3-O-xyloside) are pentosyl glycosides of quercetin and share identical deprotonated masses ($[M-H]^- = 433.0771$ Da). However, reynoutrin is sometimes referred to as a rhamnoside in certain databases, which would yield a different neutral loss of 146 Da (rhamnose) and a $[M-H]^-$ at m/z 447.0927, not observed in this spectrum.

The calculated deprotonated mass for $C_{20}H_{18}O_{11}$ is 433.0771 Da, matching the observed precursor ion at m/z

433.0758 with a mass error of only 0.0013 Da, indicating the exceptional agreement. Hence, based on the accurate precursor mass, the characteristic neutral loss of 132 Da indicative of a pentose sugar, and the diagnostic quercetin aglycone fragment at m/z 301, the compound is conclusively identified as avicularin (quercetin 3-O-arabinofuranoside).

The mass spectrometry (MS/MS) analysis of the compound was performed in negative electrospray ionization (ESI⁻) mode, revealing a prominent precursor ion at m/z 417.0817 (Fig. 9), corresponding to the deprotonated molecular ion $[M-H]^-$. The fragmentation spectrum showed a characteristic and significant neutral loss of 132.0431 Da, resulting in a base peak at m/z 285.0386. This mass difference aligns precisely with the molecular weight of a pentose sugar (calculated mass for $C_5H_8O_4 = 132.0423$ Da), revealing that the compound is a pentosyl glycoside and that the fragment at m/z 285.0386 represents the deprotonated aglycone. To identify aglycone, the neutral mass was calculated as $285.0386 + 1.0078 = 286.0464$ Da. This value matches closely with the monoisotopic mass of Kaempferol ($C_{15}H_{10}O_6$; calculated mass = 286.0477 Da), with a minimal mass error of 0.0013 Da, confirming its identity. Combining the identified aglycone (kaempferol) with the observed pentose sugar loss, the overall molecular formula was determined to be $C_{20}H_{18}O_{10}$, yielding a calculated neutral monoisotopic mass of 418.0900 Da. The theoretical deprotonated mass ($[M-H]^-$) is thus $418.0900 - 1.0078 = 417.0822$ Da, which matches the observed precursor ion (m/z 417.0817) with an excellent mass accuracy (error of 0.0005 Da). The compound is consistent with juglanin (kaempferol 3-O- α -L-arabinopyranoside) or kaempferol 3-arabinofuranoside, both of which are structural isomers sharing the same elemental composition ($C_{20}H_{18}O_{10}$) and characteristic pentose loss. Differentiation between these isomers requires complementary techniques such as chromatographic retention time comparison with authentic standards or advanced ion mobility spectrometry.

In conclusion, based on precise mass measurements and the diagnostic fragmentation pattern (National Center for Biotechnology Information, 2025) showing a pentose loss and a kaempferol aglycone, the compound is conclusively identified as a kaempferol pentoside, consistent with juglanin

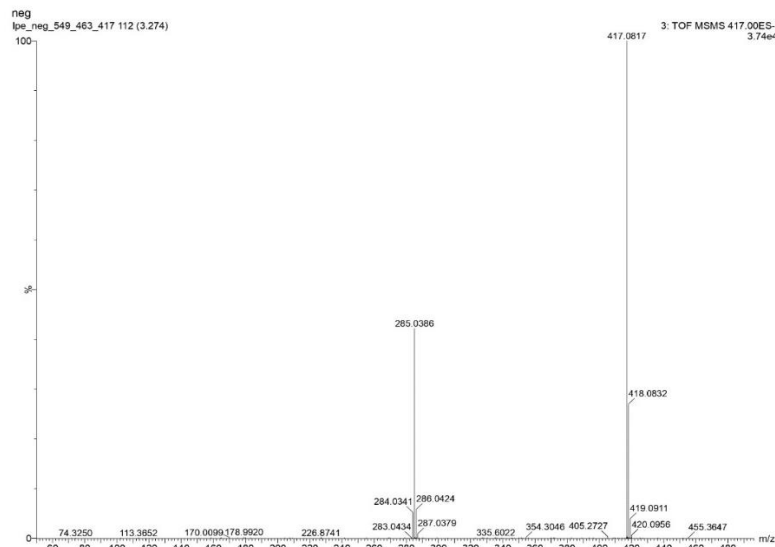


Fig. 9: MS/MS spectrum of juglanin (m/z 417.0817) identified in the ethyl acetate extract of *Entada rheedii* leaf. The spectrum shows a precursor ion at m/z 417.0817 ($[M-H]^-$) with a characteristic neutral loss of 132 Da, resulting in a major fragment ion at m/z 285.0386 corresponding to kaempferol aglycone. Additional minor fragments include m/z 284.0341, 286.0424 and 418.0832. The fragmentation pattern confirms the presence of kaempferol pentoside glycoside consistent with juglanin.

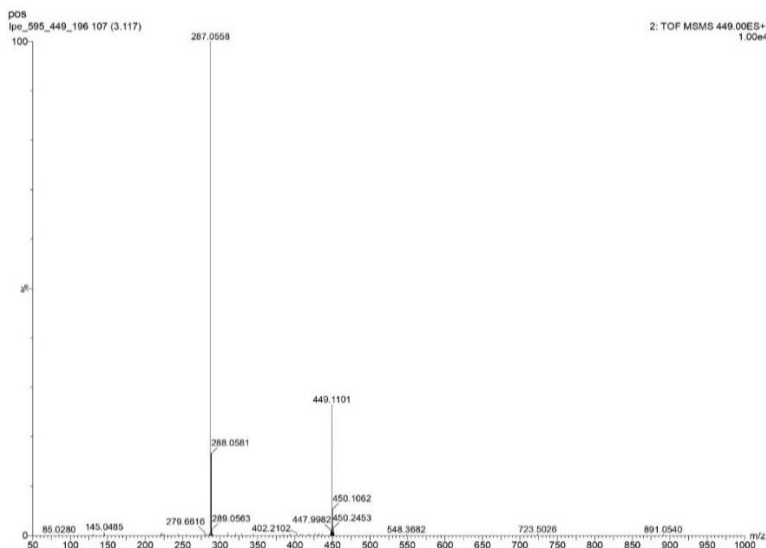


Fig. 10: MS/MS spectrum of astragalin (m/z 449.1101) identified in ethyl acetate extract of *Entada rheedii* leaf. The spectrum shows a precursor ion at m/z 449.1101 ($[M+H]^+$) with characteristic neutral loss of 162 Da, resulting in a major fragment ion at m/z 287.0558 corresponding to kaempferol aglycone. Additional minor fragments include m/z 288.0581, 450.1062, and 145.0485. The fragmentation pattern confirms it to be kaempferol-3-O-glucoside, consistent with astragalin.

or kaempferol 3-arabino-furanoside.

Astragalin presented a protonated molecular ion $[M+H]^+$ at m/z 449.1101 (Fig. 10). A major fragment ion at m/z 287.0558, resulting from the neutral loss of glucose (162 Da), unequivocally confirmed the presence of a kaempferol core (National Center for Biotechnology Information, 2024). The spectrum shows a precursor ion at m/z 449.00, acquired in positive electrospray ionization (ESI+) mode. This corresponds to the protonated molecule of astragalin ($[M+H]^+$). The most intense peak (base peak) is observed at m/z 287.0558. The base peak fragment at m/z 287.0558 corresponds to a neutral loss of 162 Da ($449 - 287 = 162$ Da) from the precursor ion. A neutral loss of 162 Da in positive ion mode is highly characteristic of the loss of a hexose sugar moiety, such as glucose, from a glycoside. This indicates that the compound is a hexosyl glycoside, and the fragment at m/z 287.0558 represents the protonated kaempferol aglycone ($[M+H]^+$ of kaempferol, m/z 286). This fragmentation is consistent with the known behaviour of kaempferol glycosides. Another significant fragment is observed at m/z 449.1101, which is likely the protonated molecular ion $[M+H]^+$, indicating the neutral molecule has a mass of 448 Da. Other minor fragments are present, including m/z 288.058, 450.106

and 450.2453. The precursor ion at m/z 449 and the dominant neutral loss of 162 Da, yielding the protonated kaempferol aglycone at m/z 287, definitively confirm the identification of the compound as astragalín (kaempferol 3-O-glucoside).

Spiraeoside was detected at m/z 463.0861 in negative ion mode (Fig. 11). Spiraeoside fragmented to m/z 301.0341, which is highly indicative of a kaempferol derivative, consistent with previous reports (National Center for Biotechnology Information, 2024). The spectrum shows a precursor ion at m/z 463.00, acquired in negative electrospray ionization (ESI-) mode. This corresponds to the deprotonated molecule of spiraeoside ($[M-H]^-$). The most intense peak (base peak) is observed at m/z 463.0861, which is the deprotonated molecular ion. This suggests that either the collision energy was relatively low, resulting in little fragmentation of the precursor, or the deprotonated molecule is extremely stable under the collision energy conditions used. A significant fragment ion is observed at m/z 301.0341. This corresponds to a neutral loss of 162 Da ($463 - 301 = 162$ Da) from the precursor ion. In negative ion mode, a neutral loss of 162 Da is characteristic of the loss of a hexose sugar moiety (e.g., glucose) from a glycoside. This indicates that the compound is a hexosyl glycoside, and the fragment at m/z 301.0341 represents the deprotonated quercetin aglycone ($[M-H]^-$ of quercetin, m/z 302). Other fragments include m/z 300.0273 and 302.0374. The compound's identity as spiraeoside (quercetin 4'-O-glucoside) is confirmed by the precursor ion at m/z 463 and the distinctive neutral loss of 162 Da, which yields the deprotonated quercetin aglycone at m/z 301.

Kaempferol-3-O-rutinoside/nitroflorin derivative displayed a precursor ion at m/z 595.1656 (Fig. 12). Fragmentation patterns produced m/z 287.0544, among other ions, strongly suggesting a kaempferol backbone or possibly breakdown products related to porphyrins. (National Center for Biotechnology Information, 2024). The spectrum shows a precursor ion at m/z 595.00, acquired in positive ESI+ mode. This corresponds to the protonated molecule of kaempferol-3-O-rutinoside ($[M+H]^+$). The most intense peak (base peak) is observed at m/z 595.1656, which is the protonated

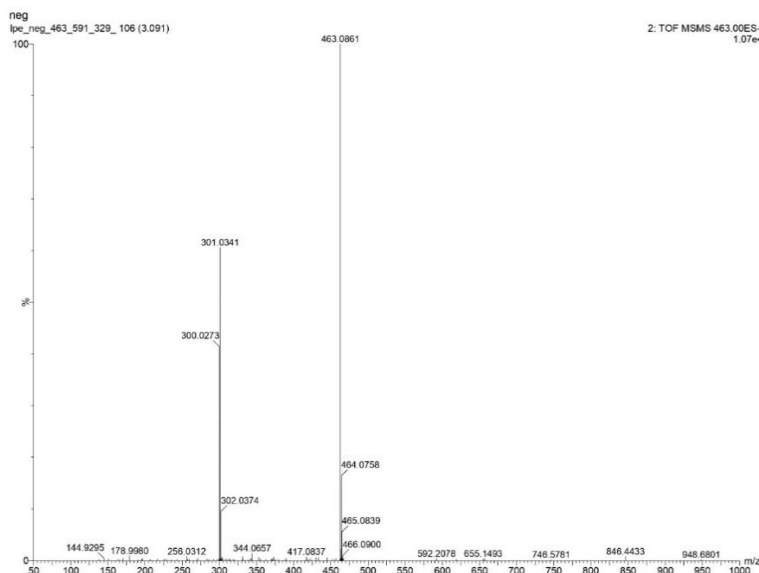


Fig. 11: MS/MS spectrum of spiraeoside (m/z 463.0861) identified in the ethyl acetate extract of *Entada rheedii* leaf. The spectrum shows a precursor ion at m/z 463.0861 ($[M-H]^-$) with a characteristic neutral loss of 162 Da, producing a major fragment ion at m/z 301.0341 corresponding to the quercetin aglycone. Additional minor fragments include m/z 300.0273, 302.0374, and 464.0758. The fragmentation pattern confirms the presence of quercetin 4'-O-glucoside, consistent with spiraeoside.

molecular ion $[M+H]^+$. This indicates high stability of the protonated molecule or relatively low collision energy, leading to less extensive fragmentation of the precursor. A significant fragment ion is observed at m/z 449.1068. This corresponds to a neutral loss of 146 Da ($595 - 449 = 146$ Da) from the precursor ion. A neutral loss of 146 Da is characteristic of the loss of a methyl pentose sugar, such as rhamnose. This suggests the initial cleavage of terminal rhamnose unit from the rutinoside.

Another significant fragment ion is observed at m/z 287.0544. This corresponds to a neutral loss of 308 Da ($595 - 287 = 308$ Da) from the precursor ion. A neutral loss of 308 Da is indicative of the loss of a

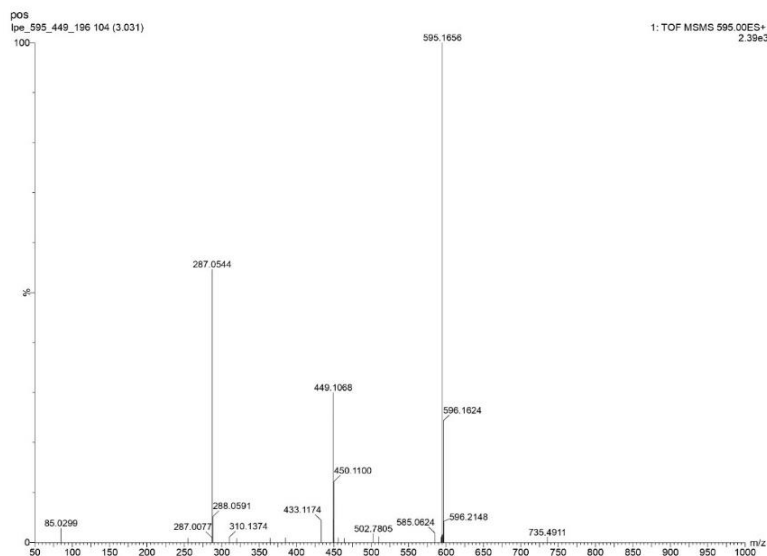


Fig. 12: MS/MS spectrum of kaempferol-3-O-rutinoside/nitroflorin derivative (m/z 595.1656) identified in the ethyl acetate extract of *Entada rheedii* leaf. The spectrum shows a precursor ion at m/z 463.0861 ($[M-H]^-$) with a characteristic neutral loss of 162 Da, producing a major fragment ion at m/z 301.0341 corresponding to the quercetin aglycone. Additional minor fragments include m/z 300.0273, 302.0374, and 464.0758. The fragmentation pattern confirms the presence of quercetin 4'-O-glucoside, consistent with spiraeoside.

disaccharide residue (e.g., glucose + rhamnose) from a glycoside. This fragment at m/z 287 represents the protonated kaempferol aglycone ($[M+H]^+$ of kaempferol, m/z 286). Other fragments include m/z 288.0591, 450.1100, and 596.1624. The precursor ion at m/z 595, coupled with the characteristic neutral losses of 146 Da (rhamnose) and 308 Da (rutinoside), leading to the kaempferol aglycone at m/z 287, strongly confirms the identification of compound as kaempferol-3-O-rutinoside.

This fragmentation pathway is highly diagnostic for rutinosides.

The comprehensive LC-QTOF-MS/MS profiling unequivocally revealed a diverse array of flavonoids and glycosides as major constituents of *E. rheedii* ethyl

acetate extract. Specifically, the identification of compounds such as genistein, kaempferol, quercetin, astragalin, and spiraeoside strongly suggests that these compound classes collectively constitute the primary active chemical signature of the extract. This observation advances beyond merely stating that “phytochemicals are present,” providing a specific understanding of the key chemical drivers of the plant's bioactivity. These identified compounds are extensively documented in the scientific literature for their wide range of potent bioactivities, including significant antioxidant, anti-inflammatory, antimicrobial, and anticancer properties (Riaz *et al.*, 2018; Nile *et al.*, 2021; Tian *et al.*, 2021). Their pharmacological effects are predominantly mediated by the collective and potentially synergistic actions of these specific flavonoids and their sugar conjugates. This provides a clear, chemically driven explanation for the plant's traditional efficacy, bridging traditional knowledge with modern scientific understanding.

Numerous studies have consistently linked flavonoids to a broad spectrum of pharmacological properties, notably anti-cancer and cardioprotective effects. Flavonoids work against cancer in a number of ways, such as by modifying the enzymes that break down reactive oxygen species (ROS), interfering with the progression of the cell cycle, triggering apoptosis and autophagy, and preventing the growth and invasion of tumor cells (Kopustinskiene *et al.*, 2020). Apigenin is a significant flavonoid recognized for its potent antioxidant and anti-inflammatory capabilities. Its effectiveness in treating a range of pathological conditions has been well-documented, operating by altering key biological activities. Its capacity to eliminate dangerous free radicals, which lowers oxidative stress, is a key component of its disease-prevention action. Additionally, by regulating pro-inflammatory cytokines, the compound's anti-inflammatory properties are essential for halting the advancement of illnesses. Evidence from both laboratory (*in vitro*) and living organism (*in vivo*) studies has also established its potential as an anti-cancer agent through its influence on cell signalling molecules (Allemailem *et al.*, 2024).

Quercetin is known to be an effective cancer chemotherapy agent and has been shown to specifically slow down the growth of tumour cells (Rather and Bhagat, 2019). Juglanin has been shown to influence numerous functional proteins either directly or indirectly, such as Nrf2, STING, NF- κ B, SIRT1, AMPK, AKT, MAPK, JAK, NLRP3, TGF- β 1, and KLF-2, among others. Through these interactions, it exhibits a wide range of effects, including anti-inflammatory, antioxidant, anti-fibrotic, anti-thrombotic, anti-angiogenic, anti-osteoporotic, hepatoprotective, hypolipidemic, hypoglycemic, and anti-apoptotic activities – although it can induce apoptosis in cancer cells. Consequently, juglanin is considered a potential therapeutic or preventive agent for various diseases and conditions such as fibrosis, metabolic syndrome, atherosclerosis, cerebral ischemia, myocardial reperfusion injury, skin injuries, neurodegenerative diseases, osteoporosis, arthritis, and multiple types of cancer (Rutkowska *et al.*, 2024).

Spiraeoside, a naturally occurring quercetin glucoside, is also reported to possess potent antitumor activity (Nile *et al.*, 2021). Kaempferol, in addition to its established anti-inflammatory and antioxidant properties, kaempferol has demonstrated significant anticancer potential through its ability to modulate various cellular processes involved in tumour development. The molecular mechanisms of action of genistein as a chemotherapeutic agent have been extensively studied across various cancer types. Genistein is known to influence apoptosis, angiogenesis, metastasis, and multiple stages of the cell cycle (Tuli *et al.*, 2019). The consistent presence and identification of these pharmacologically active compounds in *E. rheedii* strongly support its traditional medicinal use and underscore its considerable potential for further pharmaceutical exploration and development.

While LC-MS/MS spectra provided robust confirmation of molecular identities for most compounds, it is crucial to acknowledge a key limitation: the definitive distinction between certain isomeric forms (e.g., avicularin vs. reynoutrin) could not be achieved solely through MS/MS data. This limitation highlights the necessity for complementary analytical techniques, such as nuclear magnetic resonance spectroscopy or direct comparison with pure authentic standards, for unambiguous structural elucidation of such isomers. This underscores the need for further studies involving targeted compound isolation and detailed structural elucidation to fully resolve the identities of all constituents.

The present study is the first comprehensive LC-QTOF-MS report, profiling the ethyl acetate extract of *E. rheedii* leaves sourced from Kerala, India. The detailed novel phytochemical analysis provides strong scientific validation for its traditional medicinal uses by identifying a rich array of bioactive compounds, flavonoids such as apigenin, genistein and quercetin, and flavonoid glycosides such as avicularin/reynoutrin, kaempferol 3-arabinofuranoside, astragalol, spiraeoside, kaempferol-3-O-rutinoside/nitroflorin derivative, and loliolide, a monoterpene lactone. This is the first finding on the phytochemical profile of the ethyl acetate extract of *E. rheedii* leaves. This work not only supports the ethnopharmacological relevance of *E. rheedii* but also highlights its considerable potential as a valuable source of medicine. Future research should focus on detailed structural characterization, molecular docking studies, and other bioinformatics approaches, along with targeted *in vitro* and *in vivo* pharmacological investigations to comprehensively elucidate their therapeutic potential.

Conclusion: The study established the presence of pharmacologically relevant flavonoids and glycosides in the ethyl acetate extract of *Entada rheedii* leaves. These findings validate the traditional use of *E. rheedii* and offer a chemical basis for its biological activities. Future work should aim to isolate the individual constituents, perform mechanistic bioactivity assays, and explore therapeutic applications in greater depth. Bridging traditional medicine with modern techniques like LC-QTOF-MS can accelerate the discovery of novel natural products and support the development of plant-based therapeutics.

Acknowledgment: The authors gratefully acknowledge the facilities provided by Department of Botany & Biotechnology, KVM College of Arts and Science, Cherthala, Kerala, and Department of Biotechnology (DBT-FIST Sponsored Department) at Vivekanandha College of Arts and Science for Women (Autonomous), Tiruchengode, Tamil Nadu, for carrying out this work. We also extend our

sincere thanks to the Inter-University Instrumentation Center, Mahatma Gandhi University, Kottayam, Kerala, for providing access to the LC-MS QTOF instrumentation and for the technical assistance provided during the analysis.

Author's contributions: Lekshmy R. Nair - Conceptualized the research work, collected the data, analysed it, and prepared the manuscript; Mini Gopinathan - Reviewed and edited the manuscript; M. Duraipandian - Supervised and reviewed the research work, and edited the manuscript.

Conflicts of interest: The authors declare that they have no conflict of interest.

REFERENCES

- Ali, A., Bashmil, Y.M., Cottrell, J.J., Suleria, H.A.R. and Dunshea, F.R. 2021. LC-MS/MS-QTOF screening and identification of phenolic compounds from Australian grown herbs and their antioxidant potential. *Antioxidants (Basel)*, **10**(11): 1770 [<https://doi.org/10.3390/antiox10111770>].
- Allen, D.R. and McWhinney, B.C. 2019. Quadrupole time-of-flight mass spectrometry: A paradigm shift in toxicology screening applications. *Clinical Biochemistry Reviews*, **40**: 135-146.
- Allemailem, K.S., Almatroudi, A., Alharbi, H.O.A., Al-Suhaymi, N., Alsugoor, M.H., Aldakheel, F.M., *et al.*, 2024. Apigenin: A bioflavonoid with a promising role in disease prevention and treatment. *Biomedicines*, **12**: 1353 [<https://doi.org/10.3390/biomedicines12061353>].
- Colby, J.M. and Lynch, K.L. 2018. Drug screening using liquid chromatography quadrupole time-of-flight (LC-QqTOF) mass spectrometry. pp. 181-190. *In: Methods in Molecular Biology* (ed. D.R. Dekant), Humana Press, Totowa, USA.
- El Sayed, A.M., Basam, S.M., El-Naggar, E.B.A., Marzouk, H.S. and El-Hawary, S. 2020. LC-MS/MS and GC-MS profiling as well as the antimicrobial effect of leaves of selected *Yucca* species introduced to Egypt. *Scientific Reports*, **10**: 17778. [<https://doi.org/10.1038/s41598-020-74911-3>].
- Gupta, R., Sharma, A. and Kumar, V. 2023. Comprehensive phytochemical profiling of herbal extracts using LC-MS/MS. *Phytochemical Analysis*, **34**: 45-52.
- Kopustinskiene, D.M., Kornysova, O.V. and Lazutka, J.R. 2020. Flavonoids as anticancer agents: A review. *Molecules*, **25**: 1234. [<https://doi.org/10.3390/molecules25051234>].
- Long, T., Gu, R., Linghu, C., Long, J., Kennelly, E.J. and Long, C. 2023. UPLC-QTOF-MS-based metabolomics and chemometrics studies of geographically diverse *Acer truncatum* leaves: A traditional herbal tea in Northern China. *Food Chemistry*, **417**: 135873. [<https://pubmed.ncbi.nlm.nih.gov/36933422/>].
- Nair, L.R. and Balasubrahmanian, M. 2023. Correlation between phytochemicals and antioxidant activities of different leaf extracts of *Entada rheedii*. *Journal of Plant Science Research*, **39**: 199-208.
- National Center for Biotechnology Information 2025. *PubChem Compound Summary for CID 5280443, Apigenin*. Retrieved on July 25, 2025 from <https://pubchem.ncbi.nlm.nih.gov/compound/Apigenin>.
- National Center for Biotechnology Information. 2024. *PubChem Compound Summary for CID 5282102, Astragalin*. Retrieved on October 6, 2024, from <https://pubchem.ncbi.nlm.nih.gov/compound/Astragalin>.
- National Center for Biotechnology Information. 2024. *PubChem Compound Summary for CID 5490064, Avicularin*. Retrieved on October 13, 2024, from <https://pubchem.ncbi.nlm.nih.gov/compound/Avicularin>.
- National Center for Biotechnology Information. 2024. *PubChem Compound Summary for CID 5280961, Genistein*. Retrieved on October 6, 2024, from <https://pubchem.ncbi.nlm.nih.gov/compound/Genistein>.

- National Center for Biotechnology Information. 2025. *PubChem Compound Summary for CID 5318717, Juglanin*. Retrieved on July 25, 2025, from <https://pubchem.ncbi.nlm.nih.gov/compound/Juglanin>.
- National Center for Biotechnology Information. 2024. *PubChem Compound Summary for CID 5318767, Kaempferol-3-O-rutinoside*. Retrieved on October 13, 2024, from <https://pubchem.ncbi.nlm.nih.gov/compound/Kaempferol-3-O-rutinoside>.
- National Center for Biotechnology Information. 2024. *PubChem Compound Summary for CID 100332, Loliolide*. Retrieved on October 11, 2024, from <https://pubchem.ncbi.nlm.nih.gov/compound/Loliolide>.
- National Center for Biotechnology Information. 2025. *PubChem Compound Summary for CID 5280343, Quercetin*. Retrieved on June 7, 2025, from <https://pubchem.ncbi.nlm.nih.gov/compound/Quercetin>.
- National Center for Biotechnology Information. 2024. *PubChem Compound Summary for CID 5320844, Spiraeoside*. Retrieved on October 6, 2024, from <https://pubchem.ncbi.nlm.nih.gov/compound/Spiraeoside>.
- Nile, S.H., Nile, A. and Kim, D.H. 2021. Spiraeoside: A comprehensive review on its phytochemistry, pharmacology, and potential applications. *Food and Chemical Toxicology*, **154**: 112345. [<https://pubmed.ncbi.nlm.nih.gov/34116102/>].
- Nzowa, L.K., Barboni, L., Teponno, R.B., Ricciutelli, M., Lupidi, G., Quassinti, L. *et al.*, 2010. Rheediiinosides A and B, two antiproliferative and antioxidant triterpene saponins from *Entada rheedii*. *Phytochemistry*, **71**: 254-261.
- Rather, R.A. and Bhagat, M. 2019. Quercetin: A comprehensive review on its anticancer potential. *Anti-Cancer Agents in Medicinal Chemistry*, **19**: 145-156.
- Riaz, A., Rasul, A., Hussain, G., Zahoor, M.K., Jabeen, F., Subhani, Z., *et al.*, 2018. Astragalins: A bioactive phytochemical with potential therapeutic activities. *Advances in Pharmacological and Pharmaceutical Sciences*, **2018**(1): 9794625. [<https://doi.org/10.1155/2018/9794625>].
- Rutkowska, M., Witek, M. and Olszewska, M.A. 2024. A comprehensive review of molecular mechanisms, pharmacokinetics, toxicology and plant sources of juglanin: Current landscape and future perspectives. *International Journal of Molecular Sciences*, **25**(19): 10323 [[doi:10.3390/ijms251910323](https://doi.org/10.3390/ijms251910323)].
- Salim, K.S., Harun, A., Aziz, N.A., Daud, S. and So'ad, S.Z.M. 2024. Bioactive phytochemicals and pharmacological facets of *Entada* species in Asia: A review. *Malaysian Journal of Analytical Sciences*, **28**: 1210-1230.
- Shafaat-Al-Mehedi, M., Hasan, C.M. and Haque, M.R. 2015. Isolation of flavonoids from the bark of *Entada rheedii* Spreng. *Oriental Pharmacy and Experimental Medicine*, **15**: 347-351.
- Sharmila, A. and Selvaraj, C.I. 2024. LC-MS/MS-QTOF analysis of *Anodendron parviflorum* (Roxb.) leaves extract and exploring its antioxidant, antimicrobial, and cytotoxic potential. *Future Journal of Pharmaceutical Sciences*, **10**: 122. [<https://doi.org/10.1186/s43094-024-00695-1>].
- Sugimoto, S., Matsunami, K. and Otsuka, H. 2018. Biological activity of *Entada phaseoloides* and *Entada rheedii*. *Journal of Natural Medicines*, **72**: 12-19.
- Tapondjou, L.A., Kamanzi Atchou, G., Gatsing, D. and Tane, P. 2002. Antimicrobial and cytotoxic properties of some medicinal plants from Cameroon. *Fitoterapia*, **73**: 51-56.
- Tian, C., Liu, X., Chang, Y., Wang, R., Lv, T., Cui, C. and Liu, M. 2021. Investigation of the anti-inflammatory and antioxidant activities of luteolin, kaempferol, apigenin and quercetin. *South African Journal of Botany*, **137**: 257-264. [<https://doi.org/10.1016/j.sajb.2020.10.022>].
- Tuli, H.S., Sharma, A.K. and Kashyap, D. 2019. Genistein: A comprehensive review of its molecular mechanisms and therapeutic potential in cancer. *Frontiers in Pharmacology*, **10**: 1047. [<https://doi.org/10.3389/fphar.2019.01336>].
- Usman, M., Khan, W.R., Yousaf, N., Akram, S., Murtaza, G., Kudus, K.A., *et al.*, 2022. Exploring the phytochemicals and anti-cancer potential of the members of Fabaceae family: A comprehensive review. *Molecules*, **27**: 3863. [<https://doi.org/10.3390/molecules27123863>].